

Surface cleaning from laser-induced cavitation bubbles

Claus-Dieter Ohl,^{a)} Manish Arora, Rory Dijkink, Vaibhav Janve, and Detlef Lohse
Faculty of Science, Physics of Fluids, University of Twente, 7500 AE Enschede, The Netherlands

(Received 26 April 2006; accepted 28 June 2006; published online 14 August 2006)

When bubbles expand and collapse close to boundaries, a shear flow is generated which is able to remove particles from the surface, thus locally cleaning it. Here the authors demonstrate experimentally with microparticle tracking velocimetry that the strongest forcing of particles occurs during a very brief time interval of the bubble oscillation period. During this interval a jet flow impacts and spreads radially along the surface, thus transporting the particles with it. © 2006 American Institute of Physics. [DOI: 10.1063/1.2337506]

The study of the flow induced from cavitation bubbles oscillating close to a surface is motivated by the ability of the bubbles to remove attached dirt particles, thus cleaning the surface. An example of the cleaning ability of a bubble is presented in Fig. 1. Here, the surface is covered with a thin layer of grease (Vaseline) mixed with colored particles serving as dirt particles. The left image in Fig. 1(a) depicts the surface before it is exposed to a single cavitation bubble. After the bubble oscillation has ceased, a disk shaped area with a diameter of approximately 0.4 mm is cleared from the grease-particle mixture, see center image in Fig. 1(a). After a second bubble has collapsed at the same location, the cleaned area is enlarged and most of the small grease islands having remained after the first bubble collapse are now also removed (right image of Fig. 1).

Although cavitation bubble dynamics close to surfaces is studied now for decades numerically¹ and experimentally,² yet the flow along on the surface has not been investigated in greater detail. In this letter the mechanism of acceleration of particles close to the surface is experimentally determined by correlating the bubble dynamics with the particle motion.

The bubbles in the experiments are generated by focusing an intense laser pulse from a *Q*-switched neodymium-doped yttrium aluminium garnet laser (1064 nm wavelength with 6 ns duration and 15 mJ laser energy) with an aberration minimized lens system from above into a water filled cuvette. A microscope slide built into the bottom of the cuvette serves as the material surface.

The bubble dynamics close to a boundary is recorded from the side with a high speed camera at a framing rate of 112 500 frames/s (resolution of 128 × 64 pixels) and selected frames are depicted in Fig. 2(a). The boundary is located at the bottom of each frame. We can classify the bubble motion into four dynamical stages which are represented by the individual rows of Fig. 2(a). The four stages from top to bottom are bubble expansion, bubble collapse, jetting, and the reexpansion of the bubble. Initially, the bubble expands within 100 μs to its maximum diameter of 2 mm. Due to the proximity to the boundary the bubble flattens at the bottom. Thus it obtains a nonspherical shape at maximum expansion. During shrinkage the upper more curved part of the bubble develops a liquid jet flow^{3,4} through the center of the bubble towards the rigid boundary causing the mushroomlike shape at time of 213 μs in Fig. 2. This jet flow impacts between

204 and 213 μs onto the boundary. The minimum volume of the bubble is reached around 216 μs after bubble creation. The bubble then reexpands with a roughened surface and a structure consisting of microbubbles pointing upwards.⁵

The jet flow inside the bubble originates from a flow focusing mechanism.³⁻¹⁰ In Fig. 2(b) the jet is visualized with diffuse stroboscopic illumination. The left frame depicts the bubble at time of 204 μs with the jet crossing through the center of the bubble. The jet impact on the boundary is photographed in the right frame of Fig. 2(b). Here, the jet has penetrated through the lower bubble wall and is surrounded by an annular ring, presumably a vapor and gas mixture. The velocity of the jet at impact is estimated from these two frames to be approximately 40 m/s.

The flow tangential and very close to the surface is studied with streak images from fluorescent particles (8 μm in diameter, red fluorescent polymer microspheres, Cat. No. 36-3, Duke Scientific Corp., Palo Alto, CA, USA, density of 1.19 × 10³ kg/m³). Here, the particles are not embedded in a grease matrix but sediment freely onto the microscope slide. Therefore, they are injected gently into the liquid about a minute before the experiment to allow for their settling.

The fluorescence is excited with a 50 W mercury lamp from below. Excitation and imaging of the particles are done with a 5× microscope objective on an inverted microscope (Axiovert CF40, Zeiss GmbH, Göttingen, Germany). The excitation light (green) is separated from the fluorescent image (red) with a dichroic mirror and a long pass filter. An additional laser line filter just below the microscope slide protects the microscope optics. The particle trajectories are recorded with a sensitive camera (Sensicam QE, PCO GmbH, Kelheim, Germany, 1280 × 1024 pixels). Therefore, the camera is opened for a variable time at specific moments of the bubble dynamics. Due to the low light level four neighboring pixels are summed up, thus reducing the optical resolution to 5 μm per pixel. By this method we obtain for a single cavitation bubble streak images from approximately 100–500 particles. A timing unit controls the start of the recording, the exposure duration, and the trigger of the laser.

Figure 3 depicts an example of particle streaks for the four stages corresponding to the rows of Fig. 2. The bright spot in the center is due to the plasma emission during the bubble creation and marks the center of the bubble projected onto the surface. During expansion the particles move approximately a similar distance over the exposure time of 100 μs outwards [Fig. 3(a)] as they move inwards [Fig. 3(b)] during shrinkage. Thus volume pulsation does not produce

^{a)}Electronic mail: c.d.ohl@utwente.nl

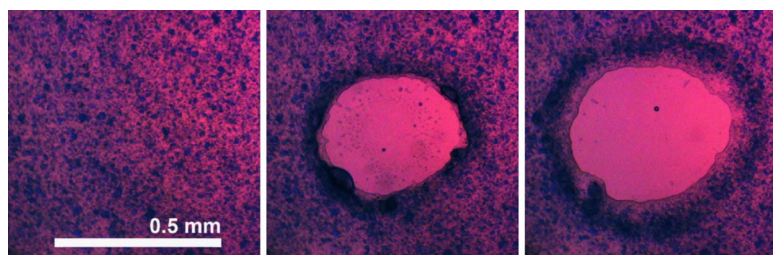


FIG. 1. (Color online) Layer of grease mixed with colored particles before (left frame) and after (center frame) it has been exposed to a cleaning bubble. The rightmost frame depicts the surface after a second bubble has been generated at the same location. Thereby, some remains of the grease from the first shot are removed and the size of the cleaned area is enlarged.

considerable transport of the particles. However, after the impact of the jet [Fig. 3(c)] all particles become largely displaced and the center region is cleared completely from particles, see Fig. 3(d).

The averaged velocities during the different stages of the bubble dynamics are quantitatively analyzed by measuring the streak lengths from the images. Figure 4 presents the modulus of the averaged velocity plotted as a function of the initial distance from the center $r=0$. In the expansion and collapse stages (from 0 to 100 μs and from 100 to 200 μs , respectively) the maximum of the averaged radial velocities is around ± 1 m/s with positive velocities during expansion and negative during shrinkage. The velocity drops to zero for $r=0$ which is plausible as the center is a stagnation point. Only during the time interval of the jet impact and radial spreading (200–230 μs) considerably higher particle velocities of 10 m/s are found. The highest velocities are reached very close to the region of jet impact. In the streak images 30 μs later (230–260 μs) all particles within a distance of 0.9 mm from the center are washed away, demonstrating that it is the induced jet flow which is responsible for the cleaning effect.

In conclusion, we have found that the most prominent boundary layer flow on the substrate occurs when the jet flow spreads radially on the surface. It is this relatively short time interval where the highest shear stress is exerted and the surface becomes cleaned. Possibly, a similar cleaning mechanism might be responsible in an ultrasonic water bath. There, many bubbles are driven into resonant pulsations by continuous acoustic waves. When they are driven to large enough oscillations they can undergo a violent collapse, and in the presence of a boundary they develop a jet.¹¹ Although, the lifetime of the bubble studied in this letter would correspond to a driving frequency of only a few kilohertz in an ultrasound bath, we suggest that the cleaning mechanism is similar for smaller bubbles, thus for higher and more relevant frequencies. Still, further research has to be undertaken to compare the importance of the jet induced shear flow with other proposed cleaning mechanisms.^{12–16}

This work was supported by grants from the “Stichting voor Fundamenteel Onderzoek der Materie (FOM)” and the “Nederlandse Organisatie voor Wetenschappelijk Onderzoek (NWO).”

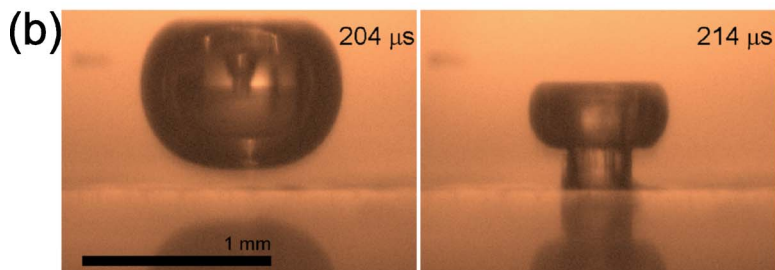
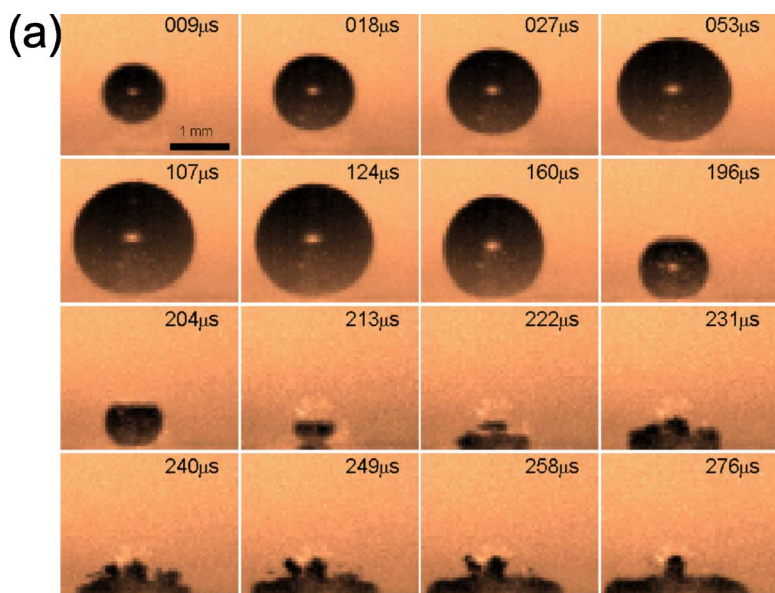


FIG. 2. (Color online) (a) Selected frames from a high-speed series of a laser-induced cavitation bubble near a boundary. The time in the upper part of each frame is the framing time of the bubble after generation with the laser. The four rows relate to four stages of the bubble dynamics: initial bubble expansion, bubble collapse, jet impact, and reexpansion. (b) Stroboscopic pictures visualizing the liquid jet within the bubble (left) and impacting on the boundary (right).

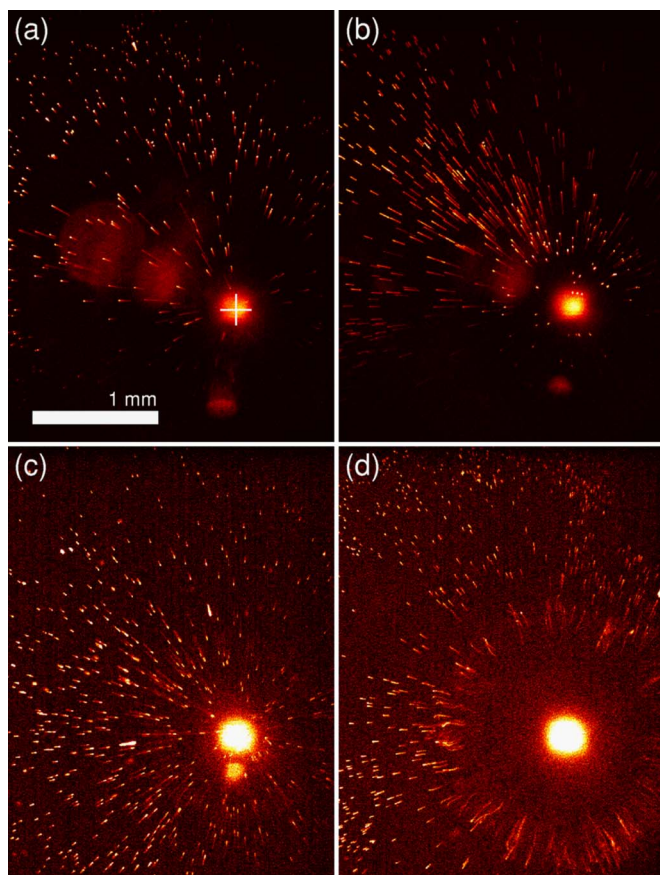


FIG. 3. (Color online) (a) Photograph of the particle streaks during the bubble expansion ($0\text{--}100\ \mu\text{s}$), (b) the bubble collapse ($100\text{--}200\ \mu\text{s}$), (c) the jet impact ($200\text{--}230\ \mu\text{s}$), and (d) reexpansion of the bubble ($230\text{--}260\ \mu\text{s}$). The position of the bubble center is indicated with a cross.

¹M. S. Plesset and R. B. Chapman, *J. Fluid Mech.* **47**, 283 (1971).

²W. Lauterborn and H. Bolle, *J. Fluid Mech.* **72**, 391 (1975).

³J. R. Blake, G. S. Keen, R. P. Tong, and M. Wilson, *Philos. Trans. R. Soc. London, Ser. A* **357**, 251 (1999).

⁴E. A. Brujan, G. S. Keen, A. Vogel, and J. R. Blake, *Phys. Fluids* **14**, 85 (2002).

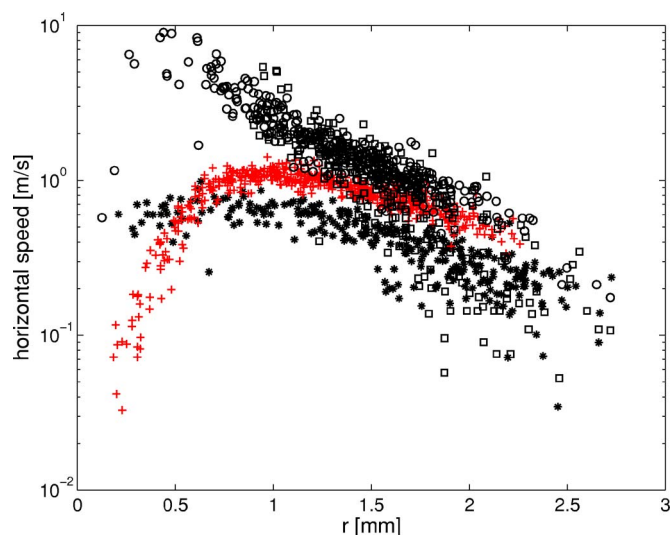


FIG. 4. (Color online) Modulus of the averaged particle velocity during the expansion (*), collapse (+), jet impact (O), and reexpansion (□) of the bubble as a function of the distance from the stagnation point at $r=0$. Note that during the collapse (+) negative velocities are recorded.

⁵O. Lindau and W. Lauterborn, *J. Fluid Mech.* **479**, 327 (2003).

⁶J. P. Dear, J. E. Field, and A. J. Walton, *Nature (London)* **332**, 505 (1988).

⁷C. D. Ohl, O. Lindau, and W. Lauterborn, *Phys. Rev. Lett.* **80**, 393 (1998); see also D. Lohse, *Nature (London)* **392**, 21 (1998).

⁸B. W. Zeff, B. Kleber, J. Fineberg, and D. P. Lathrop, *Nature (London)* **403**, 401 (2000).

⁹E. Lorenceau, D. Quere, J. Y. Ollitrault, and C. Clanet, *Phys. Fluids* **14**, 1985 (2002).

¹⁰J. M. Gordillo, A. Sevilla, J. Rodriguez-Rodriguez, and C. Martinez-Bazan, *Phys. Rev. Lett.* **95**, 194501 (2005).

¹¹P. Prentice, A. Cuschierp, K. Dholakia, M. Prausnitz, and P. Campbell, *Nat. Phys.* **1**, 107 (2005).

¹²G. W. Gale and A. A. Busnaina, *Part. Sci. Technol.* **13**, 197 (1995).

¹³E. Maisonhaute, C. Prado, P. C. White, and R. G. Compton, *Ultrason. Sonochem.* **9**, 297 (2002).

¹⁴G. W. Ferrell and L. A. Crum, *J. Acoust. Soc. Am.* **112**, 1196 (2002).

¹⁵D. Krefting, R. Mettin, and W. Lauterborn, *Ultrason. Sonochem.* **11**, 119 (2004).

¹⁶V. S. Moholkar, M. M. C. G. Warmoeskerken, C. D. Ohl, and A. Prosperetti, *AIChE J.* **50**, 58 (2004).